Parallel Variable Selection of Molecular Dynamics Clusters as a Tool for Calculation of Spectroscopic Properties

Jiří Kessler,*[a,b] Martin Dračínský,[a] and Petr Bouř*[a]

Clusters of a solute and a few solvent molecules obtained from molecular dynamics (MD) are a powerful tool to study solvation effects by advanced quantum chemical (QC) methods. For spectroscopic properties strongly dependent on the solvation, however, a large number of clusters are needed for a good convergence. In this work, a parallel variable selection (PVS) method is proposed that in some cases efficiently reduces the number of clusters needed for the averaging. The mass, charge, or atomic density MD distributions are used as a secondary variable to preselect the most probable cluster geometries used for averaging of solute spectral properties. When applied to nuclear magnetic resonance chemical shift of a model alcohol, the method allowed one to significantly reduce the total computational time, by a factor of 10. Even larger savings were achieved for the modeling of Raman and Raman optical activity spectra of (*S*)-lactamide molecule dissolved in water. The results thus suggest that the PVS method can be generally used for simulations of spectroscopic properties of solvated molecules and makes multiscale MD/QC computations more affordable.

DOI: 10.1002/jcc.23143

Introduction

Molecular dynamics (MD) provides exciting possibility to involve explicit solvent molecules in their realistic interactions and spatial distribution around a solute. If coupled with advanced quantum chemical (QC) computations, molecular properties including dynamical behavior can be obtained more realistically than using vacuum approximation or continuum solvent models. For example, vibrational properties or energy of biologically relevant systems can be modeled this way.[1,2] Similarly, modeling of solvent effects and nuclear magnetic resonance (NMR) spectroscopic properties for biologically relevant compounds required the MD solute–solvent cluster approach.[3,4] Typically, the explicit solvent is necessary for computations of the electronic excitations.[5,6] Simulation of a solvated electron and electrochemical properties probably belong to the most advanced application requiring the full explicit solvent–solute cluster models.[7–9]

In the past, we successfully used the MD cluster averaging for predictions of NMR parameters,[10,11] vibrational circular dichroism,[12] Raman optical activity (ROA),[13] or electronic excitation spectra.[14] In all these cases, the cluster approach was superior to other models.

Nevertheless, there are several obstacles hampering the cluster computations. For some properties depending on a wider molecular environment, such as NMR shielding, a periodic box may even be a better option.[10,15] For vibrational spectra simulation, proper optimization scheme had to be chosen for meaningful results.[16]

Perhaps, the most omnipresent obstacle in the MD cluster averaging is the slow convergence of the solute spectroscopic properties and consequent sharp increase of the total computational time. A combination of explicit and implicit solvent representation sometimes allows one to significantly reduce the size of the clusters, for example, by the point-charge or similar simplified solvent representations.[9,17] or by combination with advanced polarizable continuum models.[18–22] To our best knowledge, however, available procedures do not aim to reduce the number of the clusters itself. Fortunately, as shown later, a rational preselection of the clusters is possible, and it can reduce the overall computational effort significantly.

Strictly speaking, to represent the equilibrium Boltzmann distribution of solute molecules provided by a MD simulation, a large number of geometry snapshots must be taken without a preselection bias.[23] However, the knowledge of the full distribution is not necessary, if only an average value is calculated. Still, the convergence of computed properties is determined by a random noise and scales very slowly with the number of snapshots, $\sim N^{-1/2}$.[24,25] For a Raman spectra simulation, for example, the cluster computation led to a 10^5 increase of computational time if compared to a continuum solvent model.[13] Therefore, instead of a plain Boltzmann averaging, for such cases, we propose a more efficient selection of the clusters based on a solvent density distribution as a parallel variable.

The parallel variable selection (PVS) idea is outlined in Figure 1. An average of a property X, which may depend on the density ρ,

[a] *J. Kessler, M. Dračínský, P. Bouř*
Institute of Organic Chemistry and Biochemistry, Academy of Sciences, Flemingovo Náměstí 2, Prague 166 10, Czech Republic
[b] *J. Kessler*
Department of Physical and Macromolecular Chemistry, Faculty of Science, Charles University, Hlavova 8, Prague 128 40, Czech Republic
E-mail: kessler@uochb.cas.cz or bour@uochb.cas.cz
Contract/grant sponsor: Grant Agency of the Czech Republic; contract/grant number: P208/11/0105. Contract/grant sponsor: Ministry of Education of the Czech Republic; contract/grant number: LH11033 and LM2010005.

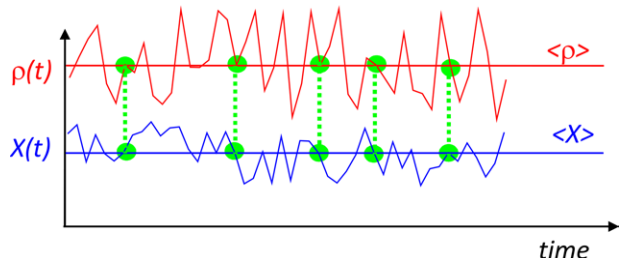

Figure 1. The PVS scheme: clusters close to the average (green) in one variable (ρ) also provide about average values of another one (X).

can be most efficiently obtained by averaging the MD snapshots that also provide ρ close to the average. In other words, we use ρ to avoid extreme cases. As X, NMR chemical shifts and Raman and Raman activity spectral intensities are calculated in this study.

It is true that the proper Boltzmann averaging including all the snapshots must be used for the density construction. However, this process involving simple manipulation of MD snapshots only is immeasurably faster than a direct computation of spectral properties by *ab initio* methods.

Methods

Model spectroscopic problems

As model systems, we used (*R*)-2,2,2-trifluoro-1-phenyl-ethanol (TPE) dissolved in (*R*)-1-phenylethanamine and the (*S*)-lactamide molecule dissolved in water (Fig. 2). For the first system, we were interested in the explicit solvent effect on NMR chemical shifts. Full outcome of these results not connected with the PVS method will be published elsewhere. The lactamide has already been taken as a model compound to investigate implicit and explicit solvent effects on Raman and ROA spectra of biologically relevant systems.[13]

The TPE molecule was placed to a cubical box (of 35.04 Å a side) filled by the (*R*)-1-phenylethanamine solvent. Program Amber[26] and the GAFF[27] force field were used for the simulations. After 1 ns equilibration a free MD propagation within the *NVT* ensemble was performed at 300 K using the 1 fs integration time step. Ten thousand snapshot geometries were generated separated by 1 ps, comprising thus 10 ns of propagation.

For the lactamide, 1000 clusters of conformer I (as defined in Ref. [13]) were selected during the Car–Parrinello MD (CPMD).[28] We chose CPMD, as it provided better spectral results than classical MD; however, there is no indication that the PVS selection would work differently for various dynamics types. Full simulation details were described earlier.[13] Briefly, periodic boxes ($10.051 \times 10.051 \times 10.051$ Å^3) containing 30 water molecules and the solute were let to propagate at 300 K, using the CPMD software,[29] 0.09676 fs integration time step, *NVT* ensemble, BLYP[30] functional, and Vanderbilt ultrasoft pseudopotentials.[31] The trajectories were saved every 50th step.

For both systems, solute–solvent clusters comprising the first solvation shells were selected from the snapshot geometries, according to the maximal distance between the solute and solvent atoms (9.0 and 3.5 Å for TPE and lactamide, respectively, cf. Fig. 2, top). The clusters were partially optimized to damp the unrealistic MD deviations for the high-frequency modes.[16] For TPE, five minimization steps were performed within Amber. For lactamide, the constraint normal mode optimization method[32,33] interfaced to Gaussian was used, with the frequency limit[16] $\omega_{max} = 300$ cm^{-1}, whereas B3LYP[30] functional, 6-311++G** basis set, and the conductor-like continuum solvent model (CPCM)[34] solvent model were

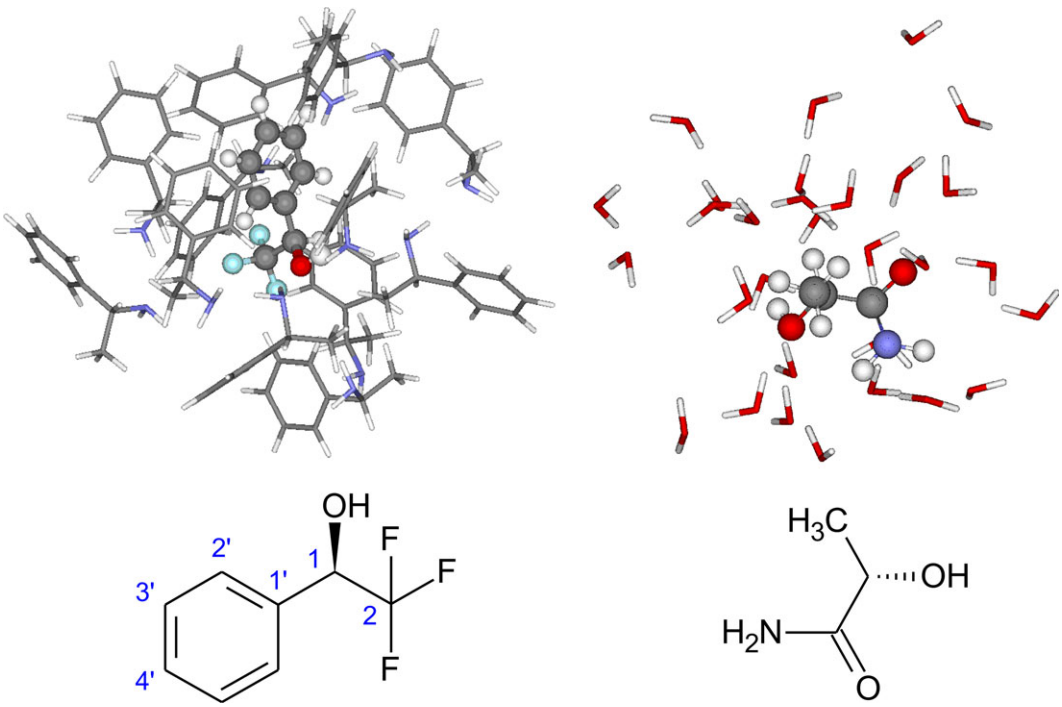

Figure 2. Model systems: TPE (left, also in an MD cluster with (*R*)-1-phenylethanamine molecules) and the (*S*)-lactamide molecule (right, with its CPMD cluster containing water molecules).

used for the remaining aqueous environment. The partial optimization does not affect the performance of the PVS method followed in this study but provides averaged results faster and closer to experiment.

QC computations

Program Gaussian09[35] was used for the computations of NMR shielding (TPE) and Raman and ROA spectra (lactamide) on the selected cluster geometries. The BPW91[36] theory was used for NMR, as the general gradient approximation (GGA) functional provides reasonably fast shielding tensors, with the 3-21G GIAO[37] basis set. The model systems well illustrate the excessive amount of computer time needed for converged results. For example, about 20,000 h in total were needed for the 10,000 shielding computations (recalculated to 2 GHz 64 bit Intel cpu). The ROA spectra were calculated at the B3LYP/6-311++G**/CPCM level of approximation, which took about 30,000 cpu h for the 1000 clusters.

To document effect of the solvent for NMR chemical shift, isotropic atomic shieldings in the TPE molecule were also calculated at the B3LYP/aug-cc-pVTZ level in vacuum and using the CPCM[34] dielectric solvent correction. As 1-phenylethanamine (relative permittivity $\varepsilon_r = 4.40$, http://www.springermaterials.com) is not supplied by Gaussian, we modeled it with butylamine ($\varepsilon_r = 4.62$). Conformer distribution obtained from MD was used instead of that based on the density functional theory (DFT) energies, as this procedure provided more faithful ROA spectra of TPE. These results were compared with the MD cluster model, comprising corrected vacuum results, that is, $\delta_{MD} = \delta_{B3LYP/aug\text{-}cc\text{-}pVTZ,single\ molecule} + \delta_{BPW91/3\text{-}21G,cluster} - \delta_{BPW91/3\text{-}21G,single\ molecule}$. For the MD clusters, the lower BPW91/3-21G level had to be used to average a large amount (10,000) of MD snapshots.

Except for TPE, similar MD trajectories and NMR data were analyzed for two other small molecules (1-phenylethanol and 1-phenylamine) in various solvents.[38] In total, 12 MD trajectories comprising each 10 million steps were included. As the performance of the PVS approach was quite similar in all cases, in this study we report only the TPE data.

Average solvent density construction

The solvent density calculated on a Cartesian grid was used as the parallel variable. First, the individual clusters selected from the MD/CPMD dynamics were rotated to achieve approximately the same positions of three selected solute atoms (C_{Phe}—$^{\alpha}$C(HO)—C for TPE and $C_{=O}$—$^{\alpha}$C(HO)—C for lactamide), by a minimization of the sum of the square distances. Then, the solvent mass, charge (atomic numbers), and atomic densities were constructed on an equidistant 0.25 Å grid surrounding the solute.

To achieve a smoother distribution, each atom occurring in a cell (*c*) contributed also to some of the 26 neighboring cells (e.g., *i*, *j*, and *k*, see Fig. 3). The density contribution was calculated as $\rho_i = \mathbf{w} \cdot \mathbf{v}_i / \mathbf{v}_i^2$ (for $i = 1$–26, **w** determines the atomic position and $\mathbf{v}_i$ is the position of cell *i* with respect to the center of cell *c*). Contribution to the cell c itself was obtained as $\rho_c = \sum_{i=1,\rho_i>0}^{26} (1 - \rho_i)/N$, where negative ρ_i values were ignored, and the number of the positive contributions $N = \sum_{i=1,\rho_i>0}^{26} 1$. We should note, however, that the smoothing finally did not have a decisive effect on the results.

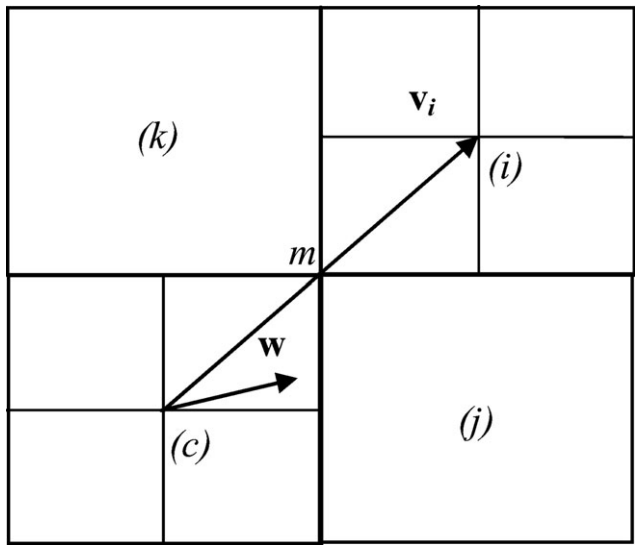

Figure 3. Construction of the density on the Cartesian grid, for an atom of a position vector **w**. The probability is distributed to the central (*c*) and the neighboring cells *i*, *j*, and *k*. For example, an atom in the middle (*m*) contributes by equal probability to *c*, *i*, *j*, and *k*, see text for the detailed formula.

The probability contribution in the 27 cells was renormalized to one (atomic density), atomic charge (nuclear charge density), or atomic mass (mass density). As another possibility, we used the density of the carbon atoms only. As shown later, the results were much dependent neither on the choice of the density type.

The cluster preselection

For each cluster selected from the trajectory, the smoothed density (ρ_c) was constructed and compared with the average density $\rho_{ave} = \sum_{c=1}^{M} \rho_c / M$, where *M* is the total number of clusters. Density farther than 7 Å from the solute was not considered to eliminate the influence of the periodic boundary conditions. Trial computations showed that reasonable variations (±1 Å, so that most of the first hydration shell is included) of this limit do not significantly influence the results. Examples of the average density distribution are plotted in Figure 4. We can see that the density clearly accumulates radially in the first solvation sphere; an angular structure is more apparent for the polar lactamide than for TPE.

A dimensionless difference was calculated as $\Delta\rho = \sum_i (\rho_{c,i} - \rho_{ave,i})\, \rho_{ave,i}\, (\sum_i \rho_{c,i}\rho_{c,i})^{-1/2} (\sum_i \rho_{ave,i}\rho_{ave,i})^{-1/2}$, where the sums run over all the grid points. Then, the clusters were sorted, starting with those exhibiting the smallest $\Delta\rho$ values.

In this way, we could compare NMR or ROA spectral properties obtained from a limited number of the preselected clusters with those obtained from the same amount of unsorted MD clusters. As a measure of agreement, all chemical shift differences with respect to the value averaged from the total of the 10,000 clusters were calculated for TPE. Similarly, for lactamide, the errors of the Raman and ROA lactamide spectra obtained from *N* clusters (S_N, $N \leq M$) were related to the exact average (S_M), using a dimensionless quantity $\delta = \int_{\omega_{min}}^{\omega_{max}} |S_N(\omega) - S_M(\omega)| d\omega / \int_{\omega_{min}}^{\omega_{max}} |S_M(\omega)| d\omega$, $\omega_{min} = 200$

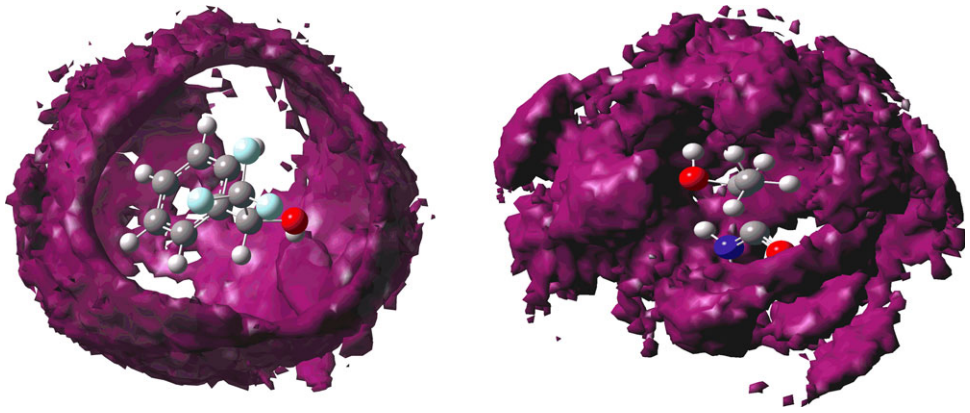

Figure 4. Mass density of the solvation shell of solvated TPE (left, a cross section, from a MD/Amber calculation) and (*S*)-lactamide (right, CPMD/BLYP). [Color figure can be viewed in the online issue, which is available at wileyonlinelibrary.com.]

cm^{-1} and $\omega_{max} = 2000\ cm^{-1}$, which proved as a good objective criterion of Raman and ROA spectral agreements in previous studies.[39–41]

Results and Discussion

PVS convergence acceleration of NMR shielding

For selected atoms, average isotropic shielding as dependent on the number of the clusters taken for the averaging is plotted in Figure 5. For all cases, the plain MD cluster averaging provides the slowest convergence, with large oscillation ($\sim\pm$0.1 ppm) even when majority of the geometries has been averaged. To exclude influence of possible correlation of MD geometries, the MD clusters were also averaged in the reversed order, which, however, provided very similar dependencies. On the contrary, the averaging based on the PVS method with the charge density provides comparatively fast and smooth convergence; typically, an error smaller than 0.1 ppm is achieved when less then one 10th (1000) of the clusters is averaged (Fig. 5, the red line). For a larger number of averaged clusters (>1000), variations of shieldings obtained using PVS are at least 10 times smaller than for the direct averaging. The slowest convergence is exhibited by the C1 and F atoms, as opposed to C2 and H1, for both the direct and the PVS methods.

In Figure 6, we compare the plain averaging and PVS based on the mass, charge, carbon, and atomic densities for the C2 atom. Clearly, all PVS variants provide faster convergence than the plain averages. The atomic density seems to provide slightly worse convergence than mass and charge, but the differences are minor in comparison to the overall improvement against the direct averaging. The behavior is similar for the subset of 1000 geometries (left part of Fig. 6) and in the full 10,000 geometry ensemble (right). Note, however, that the average value of the shielding for $N = 1000$ ($\sigma = -74.00$ ppm)

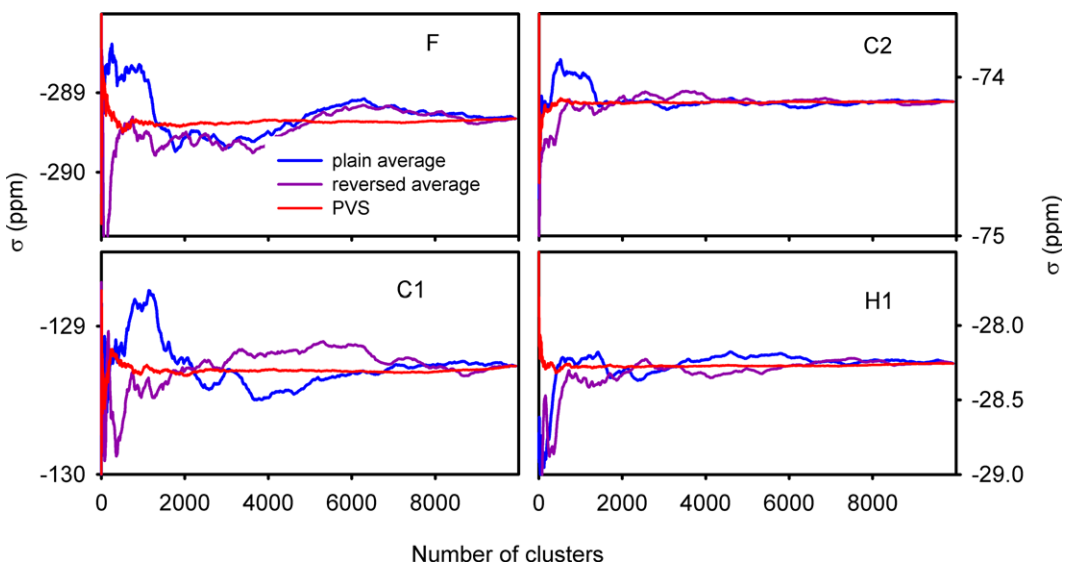

Figure 5. Isotropic shielding as a function of number of averaged clusters (for selected TPE atoms defined in Fig. 2). MD snapshots were averaged directly (in the forward and reversed orders) and using the PVS preselection based on the charge density. [Color figure can be viewed in the online issue, which is available at wileyonlinelibrary.com.]

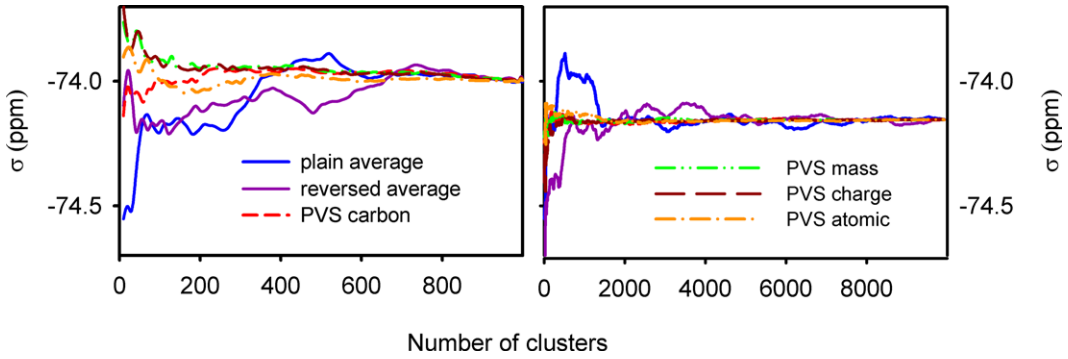

Figure 6. The C2 shielding averaging for 1000 (left) and 10,000 (right, cf. Fig. 5) MD clusters and various PVS densities. [Color figure can be viewed in the online issue, which is available at wileyonlinelibrary.com.]

differs from that for $N = 10{,}000$ ($\sigma = -74.15$ ppm). The overall quality of the simulation thus primarily depends on the total length of the MD simulation. The PVS procedure makes more effective only the extraction of the results, via reducing the number of *ab initio* computations.

Raman and ROA spectra

For the lactamide model system, the benefit of the PVS method is even more apparent than for the NMR computations. In Figure 7, the normalized errors of the ROA and Raman spectra are plotted as dependent on the number of the averaged clusters. All the density models provide very similar convergence, which is much faster than for the plain averaging. About 10× fewer clusters are needed for PVS to provide the same accuracy as the plain averaging.

In terms of detailed intensities, the spectral error for 50 CPMD snapshot averages can be judged from Figure 8, where the ROA and Raman spectra are plotted as obtained by the direct and PVS averaging and compared with the exact average. Although the direct 50 geometry average provides most of the exact spectral features, significant deviations appear in relative intensities. For Raman, the intensity is overestimated by up to 50% around 700, 1130, and 1300 cm^{-1}. The relative intensity error is even large for ROA; around 1300 cm^{-1}, even incorrect sign is obtained by the incomplete direct averaging. On the other hand, PVS provides spectral shapes quite close to the exact average.

Although the PVS method provided excellent results for the test data, it should be noted that it is an empirical method and might not be applicable in some singular cases, for example when snapshots that are far off from the average density contribute to the target property, and the property dependence on the coordinates is strong (anharmonic). Yet, we believe that for most applications the PVS tool can significantly enhance the spectral modeling.

Conclusions

In the model MD and CPMD simulations, we constructed average solvent densities, implemented the automatic preselection

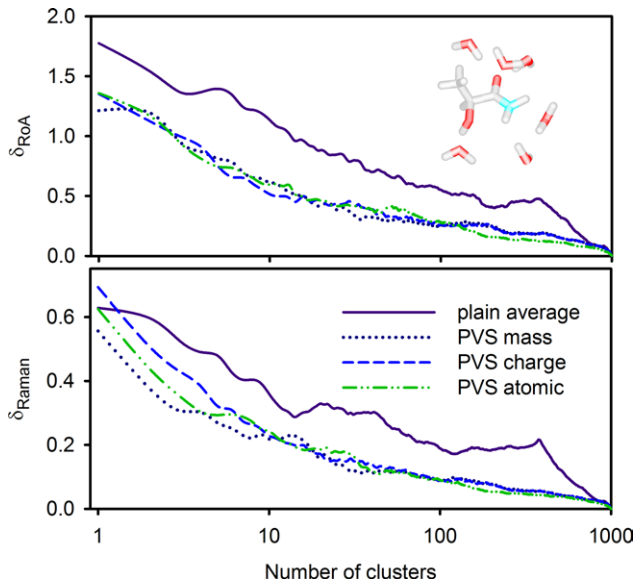

Figure 7. ROA (top) and Raman (bottom) (*S*)-lactamide spectral convergence (δ), using plain average of the CPMD clusters, and PVS with mass, charge, and atomic density. Note the logarithmic *x*-scale. [Color figure can be viewed in the online issue, which is available at wileyonlinelibrary.com.]

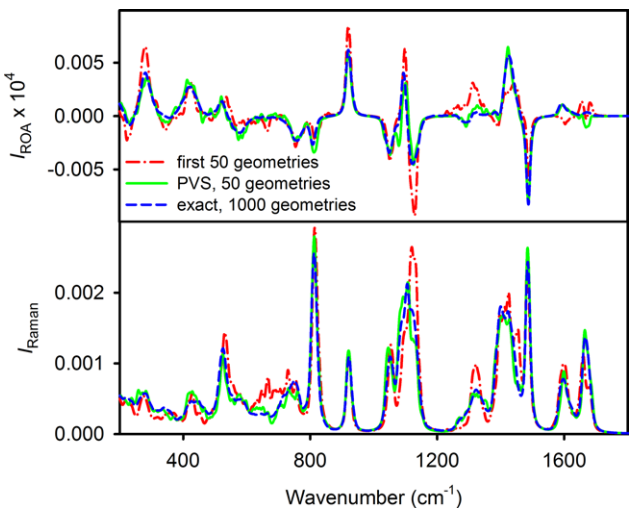

Figure 8. ROA (top) and Raman (bottom) spectra of solvated (*S*)-lactamide obtained from averaging 50 cluster or PVS (atomic density) preselected geometries and the exact 1000 CPMD geometry average. [Color figure can be viewed in the online issue, which is available at wileyonlinelibrary.com.]

of the clusters, and analyzed large amount of *ab initio* data. The results suggest that the PVS method can be efficiently used to reduce the total computational time needed for the averaging in combined quantum mechanical/molecular mechanics (QM/MM) studies. The examples were chosen to demonstrate typical computations with explicit solvent in the NMR and Raman spectroscopies. For all cases, the PVS selection proved to be significantly more efficient in comparison with the usual plain averaging. It led to about 90% savings of computer time in computations of solute spectroscopic properties. The atomic density as the parallel secondary variable at some cases provided a minor improvement over the carbon, mass, or charge densities. For the Raman and ROA spectra, a slightly faster convergence was achieved than for the NMR parameters. The PVS algorithm thus appears as a powerful tool in multiscale simulations of molecular spectroscopic properties.

Keywords: molecular dynamics · density functional theory · nuclear magnetic resonance · spectroscopy · clusters · solvent modeling

How to cite this article: J. Kessler, M. Dračínský, P. Bouř, *J. Comput. Chem.* **2013,** *34,* 366–371. DOI: 10.1002/jcc.23143

[1] J. Jeon, M. Cho, *J. Chem. Phys.* **2012**, *135,* 214504.
[2] J. Jeon, M. Cho, *New J. Phys.* **2010**, *12,* 065001.
[3] T. C. Ramalho, D. H. Pereira, W. Thiel, *J. Phys. Chem. A* **2011**, *115,* 13504.
[4] N. Faska, A. Auhmani, M. Esseffar, J. L. M. Abboud, *J. Phys. Org. Chem.* **2011**, *24,* 1209.
[5] F. DeAngelis, S. Fantacci, R. Gebauer, *J. Phys. Chem. Lett.* **2011**, *2,* 813.
[6] S. G. Neogi, P. Chaudhury, *J. Comput. Chem.* **2012**, *33,* 629.
[7] B. Abel, U. Buck, A. L. Sobolewski, W. Domcke, *Phys Chem. Chem. Phys.* **2012**, *14,* 22.
[8] O. Maršálek, T. Frigato, J. VandeVondele, S. E. Bradforth, B. Schmidt, C. Schütte, P. Jungwirth, *J. Phys. Chem. B* **2010**, *114,* 915.
[9] L. P. Wang, T. VanVoorhis, *J. Chem. Theory Comput.* **2012**, *8,* 610.
[10] M. Dračínský, P. Bouř, *J. Chem. Theory Comput.* **2010**, *6,* 288.
[11] M. Dračínský, J. Kaminský, P. Bouř, *J. Phys. Chem. B* **2009**, *113,* 14698.
[12] P. Bouř, T. A. Keiderling, *J. Phys. Chem. B* **2005**, *109,* 23687.
[13] K. H. Hopmann, K. Ruud, M. Pecul, A. Kudelski, M. Dračínský, P. Bouř, *J. Phys. Chem. B* **2011**, *115,* 4128.
[14] J. Šebek, Z. Kejík, P. Bouř, *J. Phys. Chem. A* **2006**, *110,* 4702.
[15] M. Dračínský, P. Bouř, *J. Comput. Chem.* **2012**, *33,* 1080.
[16] J. Hudecová, K. H. Hopmann, P. Bouř, *J. Phys. Chem. B* **2012**, *116,* 336.
[17] Z. Chen, G. W. Wei, *J. Chem. Phys.* **2011**, *135,* 194108.
[18] M. Caricato, B. Mennucci, J. Tomasi, F. Ingrosso, R. Cammi, S. Corni, G. Scalmani, *J. Chem. Phys.* **2006**, *124,* 124520.
[19] J. Tomasi, B. Mennucci, R. Cammi, *Chem. Rev.* **2005**, *105,* 2999.
[20] M. Caricato, F. Ingrosso, B. Mennucci, J. Tomasi, *J. Chem. Phys.* **2005**, *122,* 154501.
[21] B. Mennucci, E. Cancès, J. Tomasi, *J. Phys. Chem. B* **1997**, *101,* 10506.
[22] E. Cances, B. Mennucci, J. Tomasi, *J. Chem. Phys.* **1997**, *107,* 3032.
[23] D. A. McQuarrie, Statistical Thermodynamics; Harper and Row: New York, **1973**.
[24] L. Kaufman, D. L. Massart, In Chemometrics: Mathematics and Statistics in Chemistry; B. R. Kowalski, Ed.; D. Reidel: New York, **1984**; p. 393.
[25] B. S. Everitt. The Cambridge Dictionary of Statistics; Cambridge University Press: Cambridge, **2002**.
[26] D. A. Pearlman, D. A. Case, J. W. Caldwell, W. S. Ross, T. E. Cheatham, S. Debolt, D. M. Ferguson, G. Seibel, P. A. Kollman, *Comp. Phys. Commun.* **1995**, *91,* 1.
[27] J. Wang, R. M. Wolf, J. W. Caldwell, P. A. Kollman, D. A. Case, *J. Comput. Chem.* **2005**, *25,* 1157.
[28] R. Car, M. Parrinello, *Phys. Rev. Lett.* **1985**, *55,* 2471.
[29] CPMD Program; Max-Planck Institut and IBM Corporation: Stuttgart, **2006**.
[30] A. D. Becke, *J. Chem. Phys.* **1993**, *98,* 5648.
[31] D. Vanderbilt, *Phys. Rev. B* **1990**, *41,* 7892.
[32] P. Bouř, *Collect. Czech. Chem. Commun.* **2005**, *70,* 1315.
[33] P. Bouř, T. A. Keiderling, *J. Chem. Phys.* **2002**, *117,* 4126.
[34] A. Klamt. In The Encyclopedia of Computational Chemistry; P. R. Schleyer, N. L. Allinger, T. Clark, J. Gasteiger, P. A. Kollman, H. F. Schaefer, III, P. R. Schreiner, Eds.; Wiley: Chichester, **1998**; p.604.
[35] M. J. Frisch, G. W. Trucks, H. B. Schlegel, G. E. Scuseria, M. A. Robb, J. R. Cheeseman, G. Scalmani, V. Barone, B. Mennucci, G. A. Petersson, H. Nakatsuji, M. Caricato, X. Li, H. P. Hratchian, A. F. Izmaylov, J. Bloino, G. Zheng, J. L. Sonnenberg, M. Hada, M. Ehara, K. Toyota, R. Fukuda, J. Hasegawa, M. Ishida, T. Nakajima, Y. Honda, O. Kitao, H. Nakai, T. Vreven, J. A. Montgomery, Jr., J. E. Peralta, F. Ogliaro, M. Bearpark, J. J. Heyd, E. Brothers, K. N. Kudin, V. N. Staroverov, R. Kobayashi, J. Normand, K. Raghavachari, A. Rendell, J. C. Burant, S. S. Iyengar, J. Tomasi, M. Cossi, N. Rega, J. M. Millam, M. Klene, J. E. Knox, J. B. Cross, V. Bakken, C. Adamo, J. Jaramillo, R. Gomperts, R. E. Stratmann, O. Yazyev, A. J. Austin, R. Cammi, C. Pomelli, J. W. Ochterski, R. L. Martin, K. Morokuma, V. G. Zakrzewski, G. A. Voth, P. Salvador, J. J. Dannenberg, S. Dapprich, A. D. Daniels, O. Farkas, J. B. Foresman, J. V. Ortiz, J. Cioslowski, D. J. Fox, Program Gaussian09; Gaussian, Inc.: Wallingford, CT, **2009**.
[36] A. Becke, *Phys. Rev. A* **1988**, *38,* 3098.
[37] J. R. Cheeseman, G. W. Trucks, T. Keith, M. J. Frisch, *J. Chem. Phys.* **1996**, *104,* 5497.
[38] J. Kessler, M.S. thesis; Charles University: Prague, **2012**; pp. 1–45.
[39] M. Reiher, V. Liegeois, K. Ruud, *J. Phys. Chem. A* **2005**, *109,* 7567.
[40] S. Yamamoto, X. Li, K. Ruud, P. Bouř, *J. Chem. Theory Comput.* **2012**, *8,* 977.
[41] G. Zuber, W. Hug, *J. Phys. Chem. A* **2004**, *108,* 2108.

Received: 14 July 2012
Revised: 30 August 2012
Accepted: 7 September 2012
Published online on 10 October 2012